

doi: 10.12029/gc20160317

何垚砚,牛志军,杨文强,等.湘中南中—晚奥陶世硅质岩地球化学特征及其对奥陶纪盆地演化的启示[J].中国地质,2016,43(3): 936–952.
He Yaoyan, Niu Zhijun, Yang Wenqiang, et al. Geochemical features of middle–upper Ordovician cherts series in central–southern Hunan and their implications for basin evolution during Ordovician[J]. Geology in China, 2016, 43(3): 936–952(in Chinese with English abstract).

湘中南中—晚奥陶世硅质岩地球化学特征及其对奥陶纪盆地演化的启示

何垚砚^{1,2} 牛志军^{2,3} 杨文强^{2,3} 宋芳³ 王晓地³ 贾小辉³

(1. 中国地质大学(北京),北京 100083; 2. 中国地质调查局古生物与生命–环境协同演化重点实验室,湖北 武汉 430205;
3. 中国地质调查局武汉地质调查中心,湖北 武汉 430205)

提要:湘中南地区奥陶系由“细碎屑岩–硅质岩系–粗碎屑岩”构成,三者厚度变化具有明显的规律性;厚度等值线的展布逐渐趋于北东方向,厚度最大区域向南东方向迁移。区内岭口剖面烟溪组硅质岩 SiO_2 含量(89.08%~94.32%)和 $\text{Al}/(\text{Al}+\text{Fe}+\text{Mn})$ 值(0.52~0.79)较高,具有轻稀土略富集、无明显铈异常和铕异常的特点;大桥剖面烟溪组硅质岩 SiO_2 含量高(91.74%~95.14%), $\text{Al}/(\text{Al}+\text{Fe}+\text{Mn})$ 值为 0.34~0.56,具有轻稀土富集、无明显铕异常和间歇性铈负异常、 Y/Ho 比值低(20.65 ± 1.63)的特点。硅质岩地球化学特征及图解说明其主要为正常海相生物成因,形成于开阔的大陆边缘背景。对比邻近地区相应层位数据发现,湘中南及其邻区中—晚奥陶世硅质岩成因与沉积背景相似,指示其形成于统一盆地中,结合地层等厚度图分析认为,盆地经历了被动大陆边缘—前陆盆地的转换,硅质岩系可能是前陆盆地初始阶段的产物,在其展布范围内无明显热液影响,暗示造成华夏地块抬升的地球动力学来源可能还在该套硅质岩系展布范围的更南部或东南部。

关 键 词: 硅质岩; 地球化学; 奥陶纪; 盆地演化; 华南

中图分类号:P588.2;P54 文献标志码:A 文章编号:1000–3657(2016)03–0936–17

Geochemical features of middle–upper Ordovician cherts series in central–southern Hunan and their implications for basin evolution during Ordovician

HE Yao-yan^{1,2}, NIU Zhi-jun^{2,3}, YANG Wen-qiang^{2,3},
SONG Fang³, WANG Xiao-di³, JIA Xiao-hui³

(1. China University of Geosciences (Beijing), Beijing 100083, China; 2. Key Laboratory for Paleontology and Coevolution of Life and Environment, CGS, Wuhan, 430205, Hubei, China; 3. Wuhan Center of Geological Survey, CGS, Wuhan 430205, Hubei, China)

Abstract: Ordovician strata in central–southern Hunan consist of “finer clastic–chert–bearing series–coarser clastic rock”, and

收稿日期:2015–06–23; 改回日期:2015–09–23

基金项目:中国地质调查局地质矿产调查评价专项(12120114039301、12120113063600、1212011120117)项目资助。

作者简介:何垚砚,男,1991年生,硕士生,地层学与沉积地质学专业; E-mail:heyaoyan306@qq.com。

通讯作者:牛志军,男,1970年生,研究员,主要从事地层古生物学研究工作; E-mail:nzhijun@qq.com。

their thickness varies regularly. Spatially, the thickness contours are distributed northeastwards and meanwhile, the thickest tends to move southeastwards. In the study area, chert samples of Yanxi Formation in Lingkou section show high SiO₂ values (89.08%–94.32%) and Al/(Al+Fe+Mn) ratios (0.52–0.79), and are characterized by slight enrichment of LREE and no obvious cerium and europium anomalies. Samples of equivalent formation in Daqiao section shows high SiO₂ values (91.74%–95.14%), and the Al/(Al+Fe+Mn) ratios range from 0.34 to 0.56, with characteristics of LREE enrichment, intermittently negative cerium anomaly and no europium anomaly, and low Y/Ho ratios (20.65 ± 1.63). Geochemical characteristics and discrimination diagrams of middle–upper Ordovician cherts in central–southern Hunan indicate that these rocks were bio–genetic and formed in an open continental margin. A correlation with equivalent formation in adjacent areas shows that these cherts have similar origins and sedimentary environments, which indicates that they formed in the same basin. Combined with the analysis of the iso–thickness diagram, it could be suggested that the basin in central–southern Hunan experienced the change from passive margin to foreland basin during Ordovician, and the cherts probably resulted from this transition. In addition, there is no obvious hydrothermal activity, suggesting the geodynamics that caused the uplift of Cathaysian block might have been located to the further southern or southeastern extension range of the cherts series in central–southern Hunan.

Key words: cherts; geochemistry; Ordovician; basin evolution; South China

About the first author: HE Yao–yan, male, born in 1991, master candidate, majors in stratigraphy and sedimentary geology; E-mail: heyaoyan306@qq.com.

About the corresponding author: NIU Zhi–jun, male, born in 1970, professor, mainly engages in the study of stratigraphy and palaeontology; E-mail: nzhijun@qq.com.

Fund support: Supported by Geological and Mineral Resources Survey & Evaluation Projects of China Geological Survey (No. 12120114039301, 12120113063600, 1212011120117).

1 引言

早古生代的加里东运动是华南地质历史演化中较为重要的一幕,形成了大规模的花岗质岩浆活动、强烈的褶皱变形与区域性角度不整合^[1–2],然而对加里东期盆地性质和演化却一直存在“有洋壳”^[3–6]和“无洋壳”^[2, 7–9]之争,近年来关于华南古生代(包括早古生代和晚古生代)的一系列沉积环境与构造背景的研究成果^[10–15]促进了这一问题的研究。奥陶纪是华南早古生代盆地的重要转换时期^[1],沉积了大量的碎屑岩和硅质岩、少量的碳酸盐岩,其中含丰富笔石化石的硅质岩产于碎屑岩系之间,较为特征,易于识别,对认识早古生代沉积环境和盆地演化有重要的指示作用。常见于海洋沉积物的硅质岩是沉积盆地的特殊沉积相带,具有重要的古地理学和古海洋学意义,再加上其独特的物理化学性质,能够较好地保存成岩时的地球化学信息,推断硅质岩的成因以及形成环境,前人在这方面已经有了深入的研究,并建立了相关的对比标准及判断依据^[16–22],在沉积地质学的研究上得到了广泛的应用^[23–29]。

湘中南地区在构造上位于钦杭结合带西段,是扬子板块与华夏板块边界问题的主要争议地区,关

于其早古生代时期的盆地演化,目前主要有如下几种认识:认为华南在寒武纪—奥陶纪为扬子板块东南缘被动大陆边缘盆地^[30],在奥陶纪末—志留纪时期转变为前陆盆地^[12, 31, 32];也有学者认为华南在早古生代一直为前陆盆地^[12, 31]或一直为裂谷盆地^[33]。为此,笔者对比研究了湘中南地区奥陶世沉积记录及其中硅质岩的沉积地球化学响应,以期进一步了解华南早古生代沉积环境和构造演化。

2 地质背景

研究区位于湖南中南部,毗邻广西、广东、江西地区,生物地层区划上属于珠江盆地地理分区^[34–35],区内奥陶纪发育两套硅质岩系,分别为奥陶纪末期的五峰组和中—晚奥陶世烟溪组及其相当层位,前者不在本文的讨论范围之内。中—晚奥陶世硅质岩系在华南分布广泛,如湖南的烟溪组、双家口组,赣南的陇溪组,桂北的升坪组,其岩相类型李志明和全秋琦称之为较深水盆地型(华南型)^[35],岩性以层状黑色泥(页)岩(板岩)—硅岩型组合为特征(图5-a~d),富产笔石化石,受变质作用影响较弱,其下伏地层为桥亭子组(及其相当层位)绢云母板岩或粉砂质板岩组成的细碎屑岩(以下简称“细碎屑

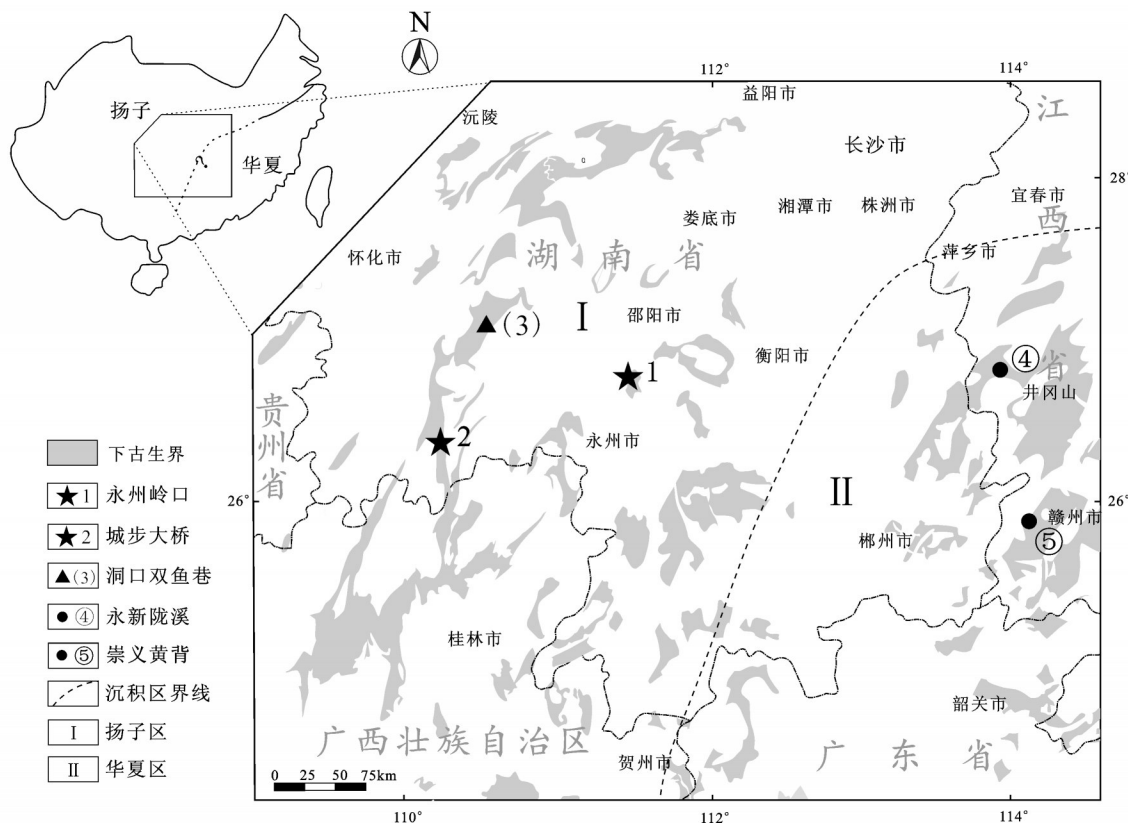


图1 研究区早古生代地层及样品分布图(岭口和大桥数据来自本文,剖面图见图4;双鱼巷数据来自文献^①;陇溪和黄背数据来自文献[23])

Fig.1 Simplified geological map showing Paleozoic strata and distribution of samples in the study area (data of section Lingkou and Daqiaois from this paper, section as shown in Fig. 4, section Shuangyuxiang from reference^①, section Longxi and Huangbei from reference [23])

岩”),上覆地层为天马山组(及其相当层位)砂岩组成的相对较粗的碎屑岩(以下简称“粗碎屑岩”)。由于岩性特殊,区域上层位亦较稳定,因此被广泛用于区域地层对比,前人在生物地层^[35~38]、沉积学^[39~41]、沉积地球化学^[23, 42]、大地构造背景^[43~44]等方面研究成果亦较为丰富。区域早古生代地层分布及地球化学样品位置图如图1所示。

3 地层学特征

3.1 区域地层对比

中一晚奥陶世烟溪组硅质岩系由于富产笔石化石,其时限较为精确。区域地层对比表如表1所示,可以看出这套硅质岩的发育具有穿时性。

3.2 硅质岩系及其上下层位厚度展布特点

古地理格局和地层厚度的空间展布均受构造

背景的制约。地层厚度的时空变化能体现盆地堆积中心^[45]的变迁,在水动力、物源等外部因素变化不大的情况下,厚度的变化往往与沉降中心的迁移有关^[45~46],为考察研究区中一晚奥陶世硅质岩的地层学特征,我们将其上下相邻层位的碎屑岩加入了对比。地层厚度数据来自区域地质调查报告以及笔者等实测剖面,为排除人为干扰,等厚度图采用surfer软件中Kriging插值法自动生成。所得的湘中南奥陶纪黑色岩系及其上下碎屑岩层位等厚度图如图2所示,由于地层出露的限制,目前只能获得控制点及其邻近范围内的残余地层等厚度图,从图中可以看出,从“细碎屑岩”(图2-a)到中一晚奥陶世硅质岩系(图2-b)再到“粗碎屑岩”(图2-c),相同地层厚度等值线北东方向的展布特点渐趋明显,堆积中心(深色区域)有往南或南东方向迁移的趋势。

^①王先辉,何江南,杨俊,等. 1:25万怀化市幅区域地质调查报告[R]. 长沙:湖南省地质调查院,2013

表1 研究区奥陶系对比(据文献[23]修改)

Table 1 Correlation of Ordovician strata of the study area (modified after reference [23])

系	统	阶	安化	隆回-城步	兴安	祁东	崇义-永新	韶关
		上覆地层	两江河组	两江河组	两江河组	跳马涧组	?	茶园山组
奥陶系	上统	赫兰特阶	五峰组	天马山组	田岭口组	天马山组	石口组	黄竹洞组
		凯迪阶	南石冲组			城步组		古亭组
		桑比阶	磨刀溪组			双家口组	韩江组	半坑组
		达瑞威尔阶	烟溪组			百马冲组		长坑水组
		大坪阶	烟溪组					
	中统	弗洛阶	桥亭子组	桥亭子组	升坪组		七溪岭组	下黄坑组?
		特马豆克阶	白水溪组					(未见底)
		白水溪组	白水溪组				爵山沟组	新厂组
		白水溪组	白水溪组				(未见底)	
		探溪组	探溪组				?	水石组
		下伏地层	探溪组	探溪组	边溪组			

注:灰色表示中—晚奥陶世硅质岩系,“?”表示因出露或研究程度等因素而尚未明确。

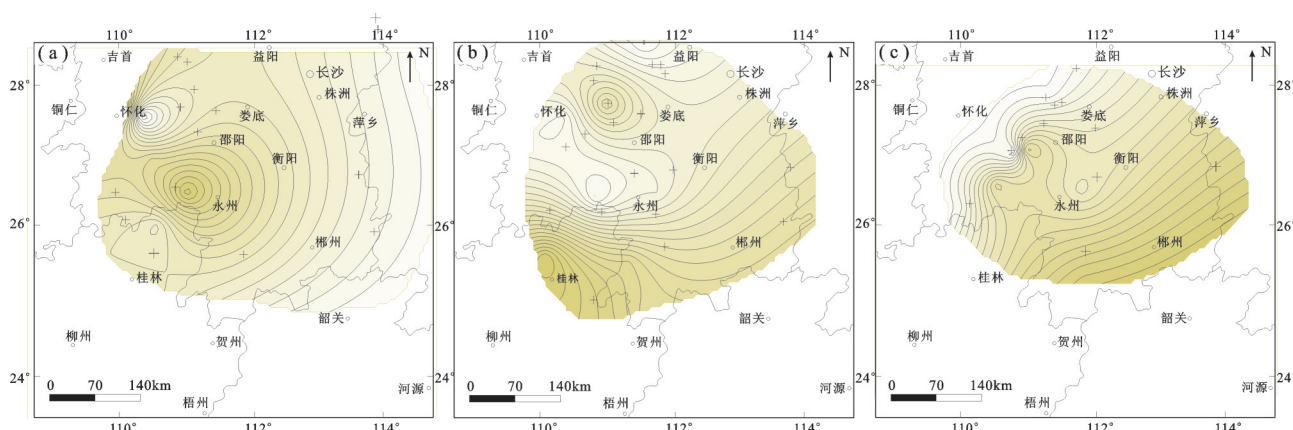


图2 湘中南中—晚奥陶世硅质岩系及其上下层位等厚度图(地层厚度资料来自1:25万区域地质调查报告和笔者实测)

a—“细碎屑岩”;b—中—晚奥陶世硅质岩系;c—“粗碎屑岩”;颜色越深厚度越大,“+”表示厚度控制点

Fig.2 Isopach map of middle–upper Ordovician cherts series and its overlying and underlying horizons in central–southern Hunan
(data of strata thickness after 1:250000 regional geological survey and measured sections)

a—Finer clastic rocks; b—Middle–upper Ordovician cherts series; c—Coarser clastic rocks; the darker the color, the thicker the strata

势^[47–48]。这些特征可以粗略代表各组地层沉积之时及之前一段时期内的盆地演化特点。

鉴于该套硅质岩的厚度展布特点以及该时期构造运动的方向性^[43],选择代表性剖面做柱状对比

如图3,可以看出这套硅质岩系由北往南(或由西北往南东)有增厚趋势,并且其中硅质岩的含量由安化—城步—兴安呈现“少—多—少”的变化趋势,表明沉积环境在这一方向(NW–SE)上有一定的变化,

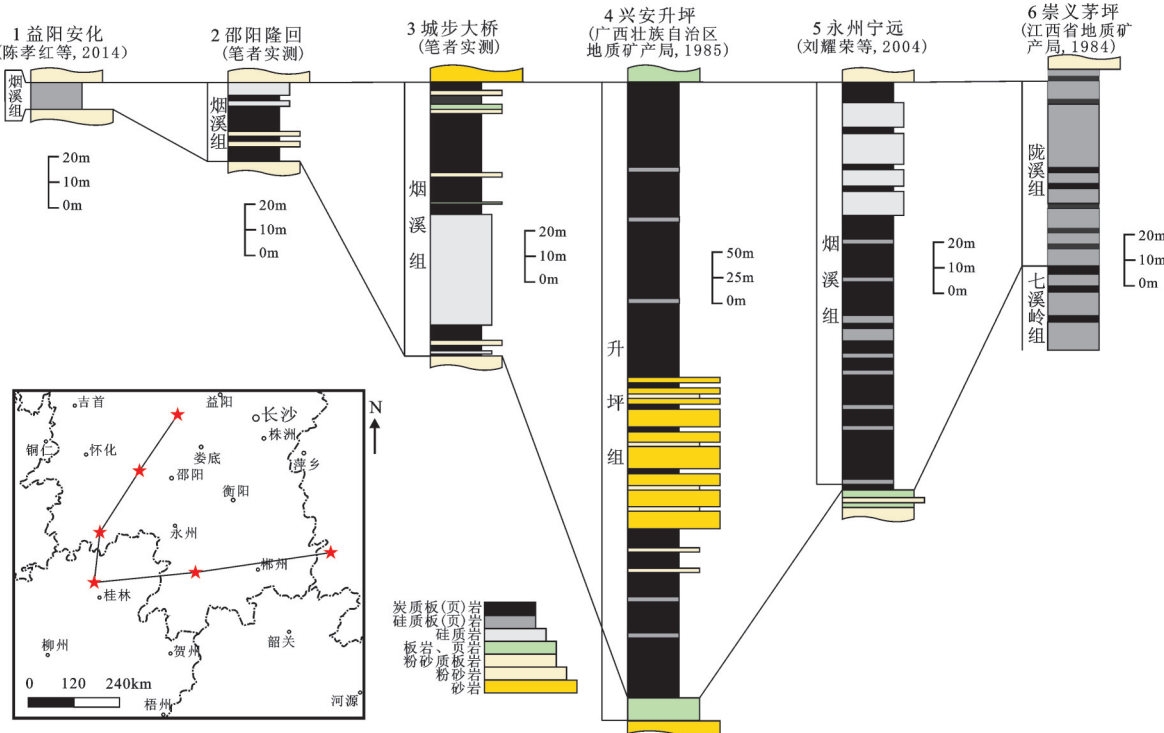


图3湘中南中—晚奥陶世硅质岩系岩石地层对比图(安化剖面据文献①,升坪剖面据文献[49],宁远剖面据文献②,茅坪剖面据文献[50])

Fig. 3 Stratigraphic correlation of middle-upper cherts series in central-southern Hunan (Anhua section after reference ①; Shengping section after reference [49]; Ningyuan section after reference ②; Maoping section after reference [50])

可能是受到了当时的古地理格局影响。

4 样品采集与测试

本文所采硅质岩样品来自城步大桥剖面和永州岭口剖面的烟溪组硅质岩(图1、图4),并引用了相邻近的洞口双鱼巷剖面烟溪组数据^③;另外为了更好地综合分析,笔者利用已发表的永新陇溪和崇义黄背剖面的陇溪组数据(据文献[23])做对比讨论。

大桥和岭口剖面样品为自底向顶采集,岩性均为薄层状硅质岩,部分样品含少量炭泥质条带(图5-g),其主量元素和稀土元素检测均在国土资源部武汉矿产资源监督检测中心完成。首先将无污染样品粉碎至200目干燥后备用,全岩主量元素在X射线荧光光谱仪(AXIOS)上测试,微量元素与稀土元素在电感耦合等离子体质谱仪(ICPMS-X Series

II)上进行分析,测试精度优于5%。文中Ce异常和Eu异常表达式分别为: $Ce/Ce^*=2 Ce_N/(La_N+Pr_N)$, $Eu/Eu^*=Eu_N/(Sm_N \times Gd_N)^{1/2}$, 稀土元素标准化均采用澳大利亚后太古代平均页岩(PASS)进行标准化^[51]。

本文所获的城步大桥和永州岭口烟溪组硅质岩主量元素、稀土元素分析结果见表2,各剖面不同环境硅质岩元素平均值及标准偏差($\pm 1\sigma$)对比表见表3。

5 地球化学特征

5.1 主量元素

城步大桥剖面样品SiO₂含量为91.74%~95.14%,平均93.51%,Al₂O₃含量为1.61%~3.03%,平均2.24%;永州岭口剖面样品SiO₂含量为89.08%~94.32%,平均92.25%,Al₂O₃含量为2.48%~5.15%,平均3.50%,其他主量元素含量均较低。对比2个剖

①陈孝红,张保民,周鹏,等. 华南中部震旦纪—志留纪地层格架、岩相古地理与成矿关系成果报告[R]. 武汉:武汉地调中心,2014.

②刘耀荣,彭学军,马爱军,等. 1:25万道县幅区域地质调查报告[R]. 长沙:湖南省地质调查院,2004.

③王先辉,何江南,杨俊,等. 1:25万怀化市幅区域地质调查报告[R]. 长沙:湖南省地质调查院,2013.

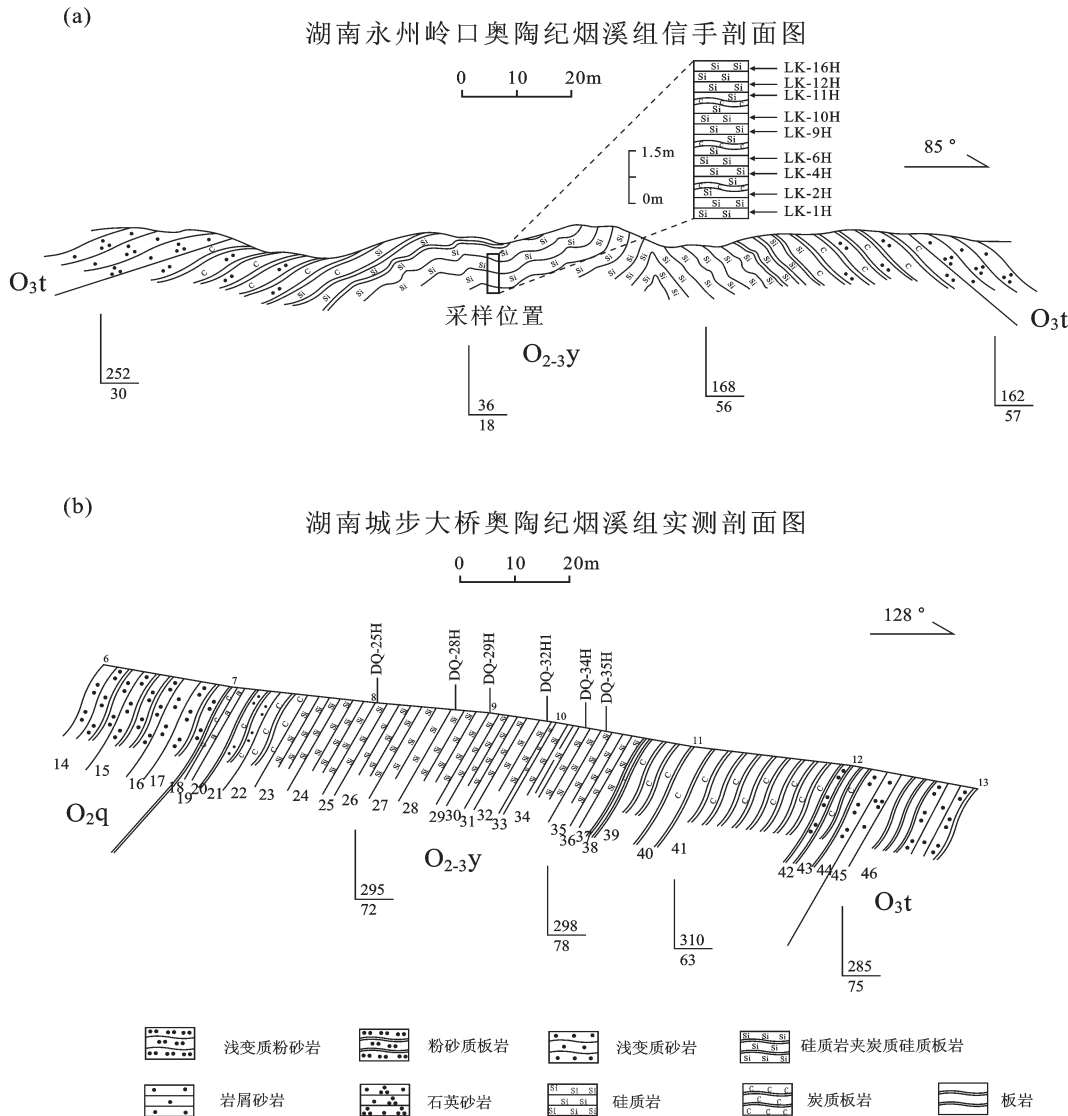


图4 中—晚奥陶世烟溪组采样剖面图(剖面位置见图1)
a—湖南永州岭口奥陶纪烟溪组信手剖面图;b—湖南城步大桥奥陶纪烟溪组实测剖面图

Fig. 4 Geological section of middle–upper cherts in Yanxi Formation(location of sections is shown in Fig. 1)
a–Sketch geological section of Yanxi Formation during Ordovician in Lingkou Yongzhou, Hunan Province; b– Geological section of Yanxi Formation during Ordovician in Daqiao Chengbu, Hunan Province

面的主量元素发现,大桥剖面样品的 SiO_2 含量高于岭口剖面,而 Al_2O_3 、 K_2O 、 Na_2O 、 TiO_2 等陆源元素的含量略低于岭口剖面,但均在仪器分析误差范围内,说明二者应属同一古地理沉积区。在PAAS和“纯硅质岩”构成的端元混合模型^[24]中,多数样品在由PASS和“纯硅质岩”组成的理论趋势线上或附近(图5),样品由含 SiO_2 80%~95%的“硅质岩”组成,反映这些硅质岩的陆源碎屑含量较低。

硅质岩中Fe、Mn的富集主要与热液的参与有关,而Al的富集则与陆源物质的介入有关。

Bostrom et al.^[52]提出,海相沉积中 $\text{Al}/(\text{Al}+\text{Fe}+\text{Mn})$ 值是衡量沉积物中热液沉积物含量的标志,Adachi et al.^[16]和Yamamoto^[17]指出这个比值在0.01(纯热液成因)到0.60(纯生物成因)之间变化。大桥、岭口硅质岩的 $\text{Al}/(\text{Al}+\text{Fe}+\text{Mn})$ 值变化范围分别为0.34~0.56,0.52~0.79。表明该套硅质岩主要为生物成因,这与样品中观察到的放射虫化石相符(图5-e~h)。

MnO/TiO_2 比值可以作为判断硅质岩来源及沉积环境的重要标志^[53],离大陆较近的边缘海等沉积环境中沉积的硅质岩, MnO/TiO_2 比值偏低,一般小

表2 永州岭口、城步大桥奥陶纪烟溪组硅质岩主量(%)及稀土(10^6)元素含量Table 2 Main element (%) and rare earth element data (10^6) of Ordovician cherts in Yanxi Formation in Lingkou, Yongzhou and Daqiao, Chengbu

分析项目	城步大桥烟溪组 (DQ-)							永州岭口烟溪组 (LK-)							
	25H	28H	29H	32H1	34H	35H	1H	2H	4H	6H	9H	10H	11H	12H	16H
SiO ₂	93.51	94.94	95.14	92.76	92.99	91.74	89.08	93.58	91.56	89.44	94.32	92.94	93.90	92.70	92.77
Al ₂ O ₃	2.73	1.61	1.66	2.41	2.00	3.03	4.29	2.65	4.12	5.15	2.99	3.03	2.48	3.56	3.21
TFe ₂ O ₃ *	1.61	2.10	1.80	2.83	2.89	2.56	3.00	1.23	1.16	1.02	0.58	1.39	1.49	0.89	1.20
CaO	0.09	0.10	0.09	0.11	0.09	0.10	0.02	0.01	0.01	0.01	0.01	0.02	0.01	0.01	0.01
MgO	0.30	0.22	0.21	0.30	0.26	0.31	0.47	0.32	0.44	0.55	0.30	0.36	0.29	0.41	0.35
K ₂ O	0.83	0.49	0.46	0.61	0.63	0.74	1.36	0.86	1.33	1.77	0.81	0.94	0.72	1.16	0.89
Na ₂ O	0.02	0.03	0.03	0.03	0.02	0.03	0.11	0.09	0.08	0.09	0.08	0.10	0.10	0.10	0.34
TiO ₂	0.11	0.07	0.07	0.11	0.10	0.15	0.18	0.11	0.19	0.29	0.13	0.15	0.09	0.18	0.14
P ₂ O ₅	0.01	0.01	0.01	0.01	0.01	0.04	0.02	0.02	0.02	0.01	0.01	0.03	0.02	0.02	0.01
MnO	0.02	0.03	0.03	0.03	0.03	0.02	0.01	0.12	0.01	0.01	0.02	0.01	0.004	0.01	0.004
LOI	0.78	0.41	0.52	0.83	1.01	1.35	2.70	1.82	1.97	3.07	1.60	1.95	1.68	2.30	2.34
Total	99.14	99.44	99.38	99.05	98.85	98.55	98.53	98.98	98.89	98.33	99.24	98.96	99.09	99.03	98.91
Al*	0.56	0.36	0.41	0.39	0.34	0.47	0.52	0.59	0.73	0.79	0.79	0.62	0.56	0.75	0.67
Al ₂ O ₃ /TiO ₂	24.82	24.77	24.41	22.31	19.42	20.07	23.83	24.09	21.68	17.76	23.00	20.20	27.56	19.78	22.93
La	7.71	3.38	6.74	8.72	7.79	11.1	7.30	4.65	9.70	9.34	7.72	8.17	3.07	6.07	6.19
Ce	14.80	3.71	12.10	15.10	8.88	18.00	15.10	9.89	19.70	20.00	15.60	16.20	6.24	11.90	14.30
Pr	1.75	0.64	1.45	1.75	1.41	2.17	1.56	1.03	2.01	2.16	1.68	1.76	0.69	1.29	1.37
Nd	6.71	2.17	5.46	6.09	4.77	7.37	5.97	3.83	7.23	8.34	6.28	6.68	2.70	4.84	5.06
Sm	1.24	0.36	1.03	1.05	0.79	1.20	1.12	0.70	1.14	1.53	1.10	1.25	0.57	0.85	0.88
Eu	0.23	0.07	0.18	0.20	0.14	0.22	0.19	0.13	0.18	0.25	0.19	0.26	0.09	0.14	0.15
Gd	1.05	0.27	0.77	0.82	0.66	0.89	0.83	0.58	0.95	1.21	0.90	0.98	0.47	0.79	0.69
Tb	0.17	0.04	0.10	0.10	0.10	0.11	0.14	0.10	0.16	0.22	0.16	0.19	0.10	0.12	0.11
Dy	0.91	0.18	0.49	0.46	0.58	0.47	0.71	0.61	0.83	1.13	0.77	1.14	0.59	0.68	0.57
Ho	0.18	0.04	0.09	0.08	0.12	0.09	0.15	0.13	0.18	0.23	0.17	0.22	0.12	0.15	0.12
Er	0.46	0.10	0.22	0.24	0.34	0.26	0.47	0.39	0.59	0.71	0.52	0.60	0.37	0.43	0.40
Tm	0.07	0.02	0.03	0.04	0.06	0.04	0.09	0.06	0.09	0.11	0.09	0.10	0.06	0.06	0.07
Yb	0.44	0.11	0.23	0.24	0.44	0.32	0.51	0.42	0.61	0.75	0.57	0.60	0.37	0.42	0.42
Lu	0.06	0.02	0.03	0.04	0.07	0.05	0.07	0.06	0.08	0.11	0.07	0.09	0.06	0.06	0.06
Y	3.83	0.68	1.79	1.60	2.78	1.86	3.93	3.28	4.73	6.34	4.52	6.12	3.23	3.48	3.25
Ce/Ce*	0.93	0.58	0.89	0.89	0.61	0.84	1.03	1.04	1.03	1.03	1.00	0.99	0.99	0.98	1.13
Eu/Eu*	0.95	1.06	0.95	1.01	0.91	1.00	0.92	0.92	0.82	0.87	0.88	1.08	0.83	0.78	0.89
(La/Yb) _{PAAS}	1.29	2.27	2.16	2.68	1.31	2.56	1.06	0.82	1.18	0.92	1.01	1.00	0.61	1.07	1.08
Y/Ho	21.28	18.89	20.11	19.05	23.17	21.38	26.55	25.43	25.71	27.93	26.59	27.69	26.92	23.84	26.21
Σ REE+Y	43.59	13.04	33.96	40.10	31.71	48.44	38.14	25.85	48.18	52.43	40.33	44.36	18.72	31.28	33.65

注: Al*=Al/(Al+Fe+Mn); Ce/Ce*=2 Ce_n/(La_n+Pr_n); Eu/Eu*=Eu_n/(Sm_n×Gd_n)^{1/2}。

于0.5,而远离大陆的大洋环境中的硅质沉积物的MnO/TiO₂比值却较高,可达0.5~3.5。除岭口LK-2号样品的MnO/TiO₂比值达到1.09外,其余样品的MnO/TiO₂值为0.01~0.43,表明这套硅质岩主体位于大陆沉积体系之下,而LK-2号样品则可能是其中的MnO受到了成岩过程的影响^[18]。

5.2 稀土元素

大桥和岭口剖面样品稀土元素总量 Σ REE值变化范围分别为 12.36×10^{-6} ~ 46.58×10^{-6} , 15.49×10^{-6} ~

46.09×10^{-6} 。大桥剖面具铈负异常,除样品DQ-28H和DQ-34H存在明显铈负异常外(Ce/Ce*值分别为0.58、0.61),其余样品Ce/Ce*值范围为0.84~0.93,岭口剖面样品具不明显的铈正异常,Ce/Ce*值分别为0.98~1.13;大桥剖面Eu/Eu*值在0.91~1.06范围内,平均值为0.98;岭口剖面Eu/Eu*值范围为0.78~1.08,平均值为0.89。可以看出,相对而言,大桥剖面的Ce较为亏损,而岭口剖面的Eu较为亏损。样品的稀土元素PAAS标准化分布曲线如图7-a,除

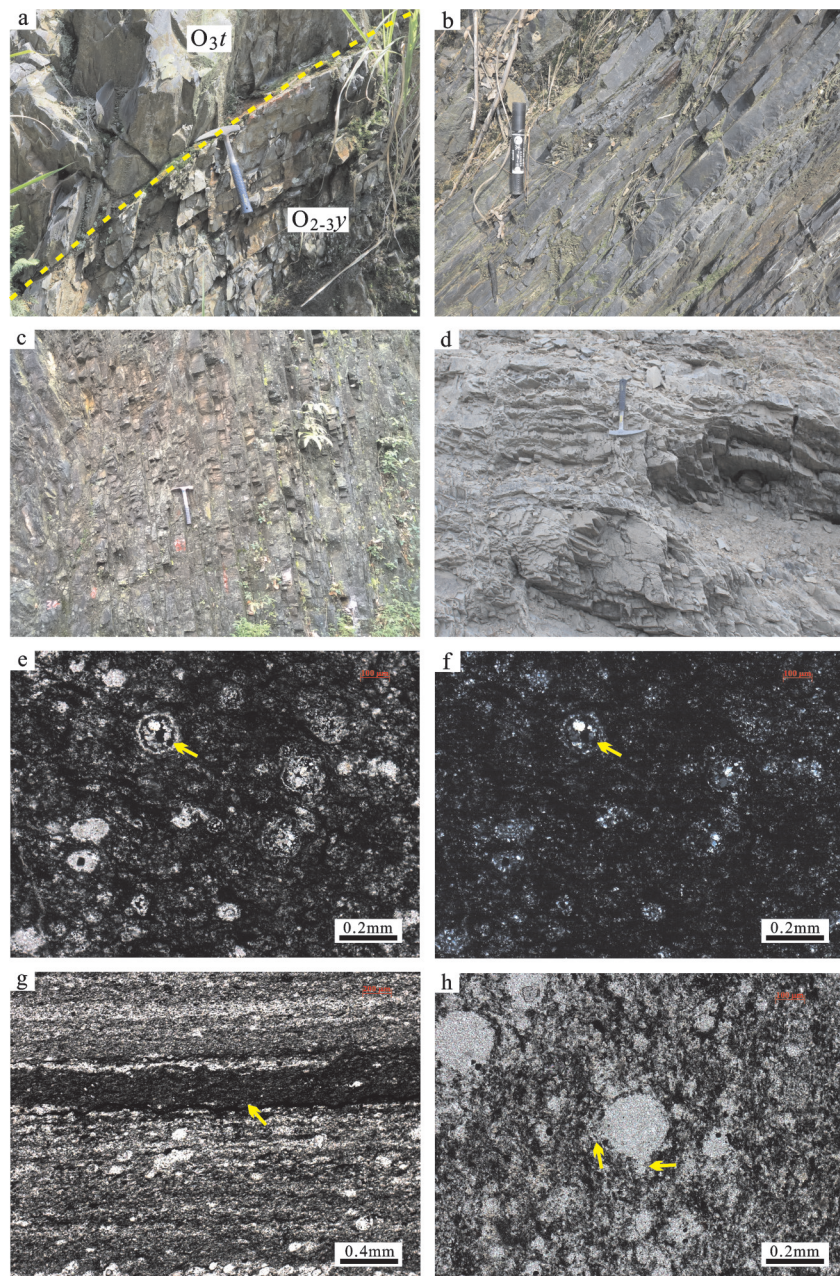


图5 湘中南中—晚奥陶世硅质岩野外露头及镜下照片

a—隆回杉木湾剖面烟溪组($O_{2-3}y$)与天马山组(O_3t)整合接触(剖面位置见图3); b—隆回杉木湾剖面中的硅质板岩夹硅质岩;
c—大桥剖面烟溪组层状硅质岩露头; d—岭口剖面烟溪组硅质岩露头; e—岭口剖面样品LK-13放射虫硅质岩, 局部被炭泥质充填(箭头所示), 单偏光; f—与e图同视域, 正交偏光; g—大桥剖面样品DQ-34中的炭质条带(箭头所示); h—大桥剖面样品DQ-28中的放射虫硅质岩,隐约可见放射虫的刺(箭头所示)

Fig. 5 Field outcrop and microscope photographs of middle–upper cherts series in central–southern Hunan

a-Conformable contact between Yanxi and Tianmashan formation in Shanmuwan section (profile position in Fig. 3); b–Siliceous slate bedding cherts in Shanmuwan section; c–Bedded cherts of Yanxi Formation in Daqiao section; d–Cherts of Yanxi Formation in Lingkou section;

e– Radiolarian cherts of sample LK-13, partly filled with carbon–argillaceous matter (indicated by arrows), plainlight;

f–The same vision field as photo e, crossed nicols; g–Carbonaceous stripes in sample DQ-34 (indicated by arrows);

h–Radiolarian cherts in sample DQ-28 with vaguely seen radiolarian thorn

岭口剖面 LK-2H、LK-11H 两个样品出现较为明显的右倾外($(La/Yb)_{PAAS}$ 比值分别为 0.82、0.61),其余样品曲线呈平坦或右倾状, ($(La/Yb)_{PAAS}$ 比值变化范围为 0.92~2.68, 反映轻稀土相对富集, 相对于邻近剖面而言(图 7-b), 大桥和岭口剖面硅质岩的稀土元素含量略低于周边地区。大桥剖面 Y/Ho 值为 18.89~23.17, 岭口剖面 Y/Ho 值明显高于大桥剖面的 Y/Ho 值, 介于 23.84~27.93。反映大桥和岭口的硅质岩可能是大陆边缘的产物^[54]。

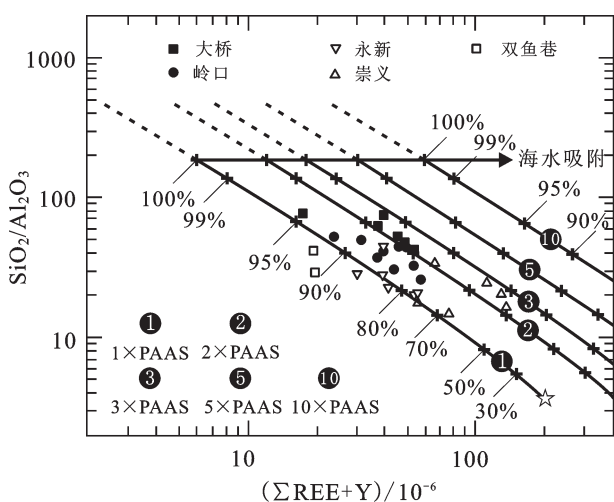


图 6 湘中南地区中—晚奥陶世硅质岩($\Sigma REE+Y$)— SiO_2/Al_2O_3 图解(底图据文献[25])

Fig. 6 ($\Sigma REE+Y$)— SiO_2/Al_2O_3 diagram of middle-upper Ordovician cherts series in central-southern Hunan (base map after reference [25])

6 硅质岩成因及沉积背景

6.1 硅质岩成因

Adachi et al.^[16] 和 Yamamoto^[17] 在系统研究了热液成因与生物成因的硅质岩后, 认为 $Al/(Al+Fe+Mn)$ 比值由纯热液成因的 0.01 到纯生物成因的 0.6 之间变化, 并由此拟定了判别热液成因与非热液成因硅质岩的 $Al-Fe-Mn$ 三角判别图解, 指出热液成因硅质岩的投点落入富 Fe 端, 非热液成因硅质岩的投点落入富 Al 端。如图 8 所示, 湘中南硅质岩样品均位于非热液成因区及其附近, 进一步说明研究区中一晚奥陶世硅质岩为非热液成因, 结合前人^[55]及本文在硅质岩中发现的放射虫(图 5-e~h), 推断湘中南地区中—晚奥陶世硅质岩系主要为生物以及化学沉积成因。

沉积物中 Al_2O_3/TiO_2 比值受风化作用、沉积搬运、沉积作用及成岩作用的影响很小^[56~58], 而当沉积物中混合一些基性或酸性火山碎屑时, 其 Al_2O_3/TiO_2 值会发生明显变化。如图 9 所示, 在 $Al/(Al+Fe+Mn)-Al_2O_3/TiO_2$ 图解^[23] 中, 岭口剖面样品投点均落在正常海相非热液成因区(C 区)及含酸性火山碎屑非热液成因区(B 区)的边缘附近, 表明岭口硅质岩为正常海相非热液成因; 而大桥硅质岩则位于 A、B、C 三个区域之间, 鉴于其中发现的放射虫(图 5-h)以及桂北地区存在的基性岩及火山碎屑岩^[49], 推测大桥地区硅质岩主要为生物成因, 但受其南部桂北地区火山物质再循环的影响。邻近剖面的硅质岩也大多落在 C 区, 对于落入 D 区的崇义剖面 C3~

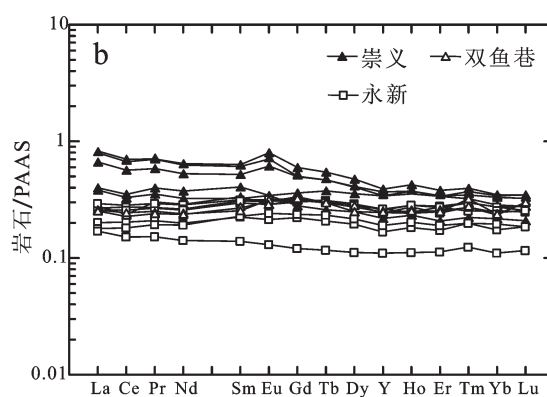
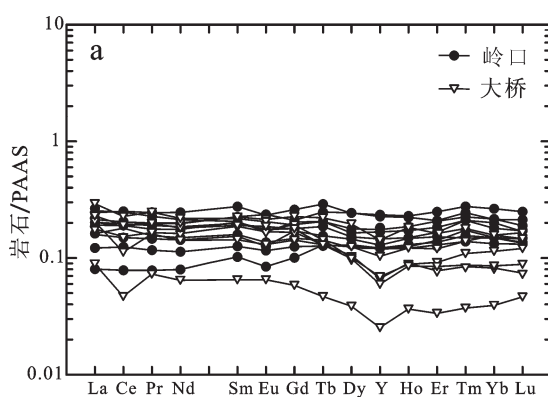


图 7 湘中南中—晚奥陶世硅质岩标准化稀土元素分配曲线^[51]

Fig. 7 PASS-normalized REE patterns of middle-upper Ordovician cherts series in central-southern Hunan

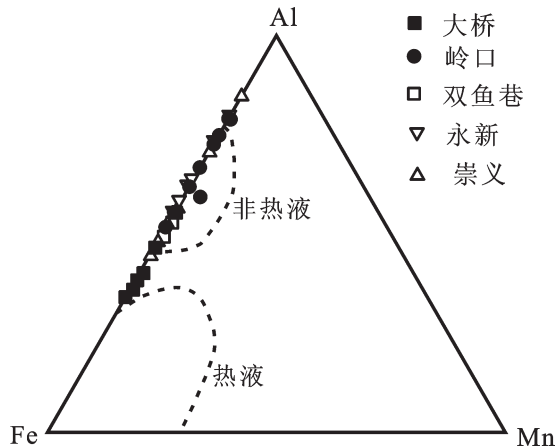


图8湘中南中—晚奥陶世硅质岩Al-Fe-Mn三角图解
(底图据文献[16])

Fig. 8 Al-Fe-Mn diagram of middle-upper Ordovician cherts series in central-southern Hunan (base map after reference [16])

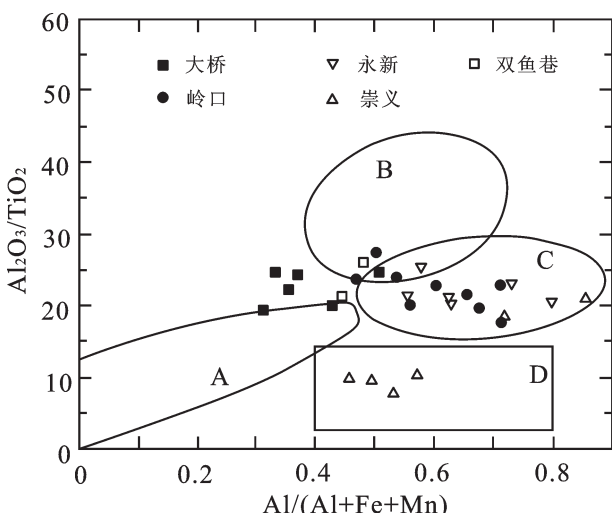


图9湘中南中—晚奥陶世硅质岩Al/(Al+Fe+Mn)-Al₂O₃/TiO₂
(底图据文献[25])

A区—基性火山热液成因硅质岩; B区—含酸性火山碎屑非热液成因硅质岩; C区—正常海相非热液成因硅质岩; D区—含基性火山碎屑非热液成因硅质岩

Fig. 9 Al/(Al+Fe+Mn)-Al₂O₃/TiO₂ diagram of middle-upper Ordovician cherts series in central-southern Hunan (base map after reference [25])

A—Hydrothermal cherts associated with basaltic volcanism; B—Non-hydrothermal cherts containing felsic volcanic clasts; C—Non-hydrothermal cherts associated with normal marine deposits; D—Non-hydrothermal cherts containing basaltic volcanic clasts

C6四个样品,张保民等研究认为是老地层中的火山物质经风化搬运后沉积在陇溪组硅质岩中造成^[23]。因此,图8和图9说明湘中南地区中—晚奥陶世硅质岩主要为正常海相生物成因,局部地区受古老基底火山物质再循环的影响。

6.2 沉积环境与构造背景

湘中南中—晚奥陶世硅质岩的Ce/Ce*、Eu/Eu*、(La/Yb)_{PAAS}、ΣREE+Y、Y/Ho平均值及标准偏差(表3)多与弗朗西斯科大陆边缘或巢湖中二叠统孤峰组的相应比值接近,说明这套硅质岩主要沉积于大陆边缘背景,但也有个别比值存在明显偏离,如大桥剖面的(La/Yb)_{PAAS}值达到了(2.05±0.61),高于表中所列的各种沉积背景,可能是受陆源物质输入的影响相对较大的原因^[59],同时,样品中ΣREE+Y值显示出比较大的变化范围,与被动大陆边缘可能包含多种构造背景信息的特点相符^[30]。

Y和Ho常具有相似的地球化学行为,平均上地壳组成及PAAS均具有和球粒陨石相似的Y/Ho值(26~28)^[56, 60]。目前,关于Y和Ho分异的报告主要集中在海水或海相碳酸盐岩^[61~63]以及河水或河流入海口^[64~65]。由于海水中Ho相对Y具有更高的移出速率,海水具有比河水及河口更高的Y/Ho值,其中河水的Y/Ho值与PAAS相近或略高于PAAS,低于海水的平均值55^[63~64]。目前低于PAAS的Y/Ho值的报告主要集中在深海铁锰结核或结壳(Y/Ho值在17~25)^[61, 66]。湘中南中—晚奥陶世硅质岩样品中,大桥硅质岩的Y/Ho值略低于弗朗西斯科远洋与弗朗西斯科洋脊的Y/Ho值(达到20.65±1.63),其余样品Y/Ho比值与美国Shoo Fly陆缘硅质岩比值接近,因此,从微量元素比值来看,湘中南中—晚奥陶世硅质岩总体上为大陆边缘背景。

Murray^[18]通过对全球早古生代至古近—新纪不同沉积背景下的硅质岩地球化学特征的详细研究,提出可用100×TFe₂O₃/SiO₂-100×Al₂O₃/SiO₂、TFe₂O₃/TiO₂-Al₂O₃/(Al₂O₃+TFe₂O₃)、TFe₂O₃/(100-SiO₂)-Al₂O₃/(100-SiO₂)和La_N/Ce_N-Al₂O₃/(Al₂O₃+TFe₂O₃)等图解来判别硅质岩的沉积环境。如图10,大桥硅质岩主要位于大陆边缘附近,仅在图10-d中落在远洋区域附近,结合其低Y/Ho比值和间歇性铈负异常的特点,说明其可能形成离大陆边缘相

表3 湘中南中—晚奥陶世硅质岩与不同环境硅质岩元素平均值及标准偏差($\pm 1\sigma$)对比^[24]Table 3 Contrast of middle–upper Ordovician cherts data in central–southern Hunan and the average value and standard deviation of chert elements in different environments^[24]

地区 / 地层	Ce/Ce*	Eu/Eu*	(La/Yb) _{PAAS}	Σ REE+Y	Y/Ho	样品数
城步大桥	0.79±0.15	0.98±0.05	2.05±0.61	31.95±11.37	20.65±1.63	6
永州岭口	1.02±0.05	0.89±0.09	0.97±0.17	36.99±10.79	26.32±1.24	9
洞口双鱼巷 [•]	0.94±0.03	1.05±0.06	1.08±0.01	56.80±1.05	27.17±0.64	2
崇义陇溪组 ^[23]	0.89±0.04	1.11±0.18	1.84±0.63	97.27±34.93	25.61±0.76	6
永新陇溪组 ^[23]	0.98±0.03	0.99±0.03	1.13±0.23	47.18±11.55	25.31±0.97	6
弗朗西斯科大陆边缘 ^[20]	1.02±0.24	1.32±0.31	0.64±0.19	66.33±54.33	23.78±2.54	15
弗朗西斯科远洋 ^[20]	0.56±0.10	1.27±0.14	1.12±0.72	63.80±49.70	21.14±3.80	4
弗朗西斯科洋脊 ^[20]	0.28±0.12	1.22±0.12	0.64±0.12	52.52±27.16	21.77±2.29	9
日本 Sasayama 远洋 ^[67]	0.73±0.25	1.12±0.10	0.87±0.29	34.71±11.18	36.80±4.58	17
巢湖中二叠统孤峰组 ^[68]	0.80±0.07	0.94±0.60	0.72±0.26	35.13±19.90	33.75±3.90	23
美国 Shoo Fly 陆缘 ^[69]	1.05±0.05	1.21±0.05	0.96±0.17	43.36±15.87	26.34±1.38	9

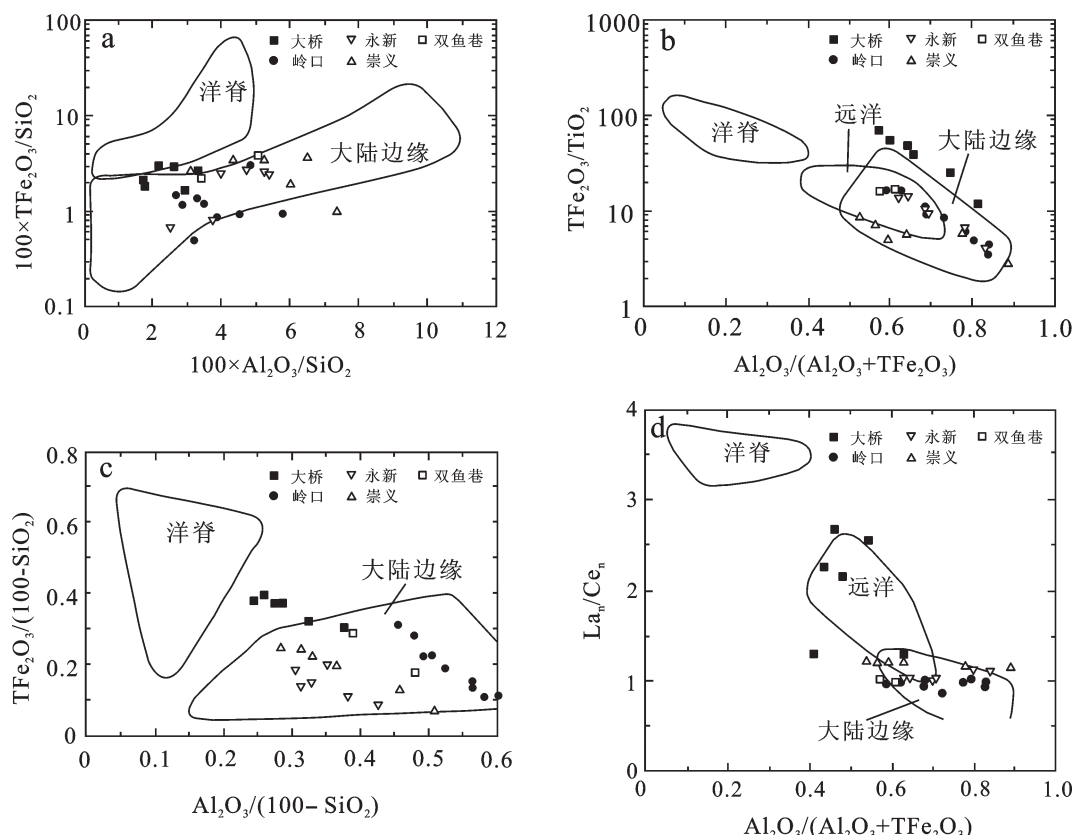


图10湘中南地区中—晚奥陶世硅质岩形成环境判别图(底图据文献[18],图例同图6)

Fig. 10 Discrimination diagrams for geological settings of middle–upper Ordovician cherts in central–southern Hunan (base map after reference [18], legends as for Fig. 6)

①王先辉,何江南,杨俊,等.1:25万怀化市幅区域地质调查报告[R].长沙:湖南省地质调查院,2013.

对较远的边缘海盆环境,受间歇性陆源物质的影响。其余硅质岩样品均落在大陆边缘及其附近区域,进一步反映湘中南及其邻区中—晚奥陶世的硅质岩总体形成于大陆边缘的构造背景。

硅质岩中REE的丰度反映了黏土矿物的组成以及被海水中的黏土或生物体吸附的情况,而 Al_2O_3 含量反映陆源黏土组分, $\text{SiO}_2/\text{Al}_2\text{O}_3$ 值代表硅化程度^[21],黄虎等^[25]建立了由PASS和“纯硅质岩”组成的 $\Sigma \text{REE}+\text{Y}$ 和 $\text{SiO}_2/\text{Al}_2\text{O}_3$ 的混合模型,用以判别沉积环境。如图6所示,曲线①②③⑤⑩分别代表相同硅化过程中硅质岩中 $\Sigma \text{REE}+\text{Y}$ 分别是PASS组分的1、2、3、5、10倍,湘中南中—晚奥陶世硅质岩的投点均落在曲线①和②之间的区域及其附近,表明该套硅质岩除了受陆源物质的影响外,还从海水中吸附了一定量的稀土元素,其中以大桥和崇义两地从海水中吸附得最多,反映这两处硅质岩形成于更开阔的海水环境。

以上各种硅质岩沉积背景投图说明,湘中南及其邻区中—晚奥陶世硅质岩总体沉积于大陆边缘的背景,为正常海相生物成因硅质岩,城步地区水体深度更大,受间歇性陆源物质输入的影响。

7 硅质岩沉积模式及对盆地构造演化的启示

湘中南及其邻区奥陶纪时期盆地的堆积中心有向南或南东方向迁移的趋势,地层的厚度展布渐趋于NE-SW方向,这与前陆盆地发育初期的演化模式有很好的对应关系,结合硅质岩地球化学特征,本文认为这是前陆盆地构造负载引起挠曲沉降形成的沉积响应,而综合硅质岩的地球化学图解以及前人研究成果^[70-72]来看,湘中南硅质岩沉积之前应为扬子东南缘被动大陆边缘盆地。据此,本文提出湘中南中—晚奥陶世硅质岩的沉积模式及其相应的盆地演化阶段(图11)如下:(1)被动大陆边缘阶段(烟溪组沉积之前):由新元古代裂谷盆地^[66]演化而来,堆积中心位于盆地中部,桥亭子组细碎屑岩形成,该阶段末期局部地段开始发育深色泥岩;(2)前陆盆地初始阶段烟溪组沉积时期:华夏地块隆升加载导致盆地挠曲沉降,盆地水深达到最大,物源供应不足,烟溪组硅质岩系作为前陆盆地初始

阶段的沉积响应开始形成,堆积中心向构造负载的一侧偏移,地层厚度展布开始表现出NE-SW方向的展布特点;(3)前陆盆地发展阶段:烟溪组沉积之后华夏地块进一步向NW阶段性^[43, 73-74]隆升,巨大的构造负载导致盆地进一步挠曲沉降,堆积中心继续向南东移动,并沉积了前陆盆地系统中的晚奥陶世天马山组(杂)砂岩,同时由于构造负载的方向性展布,地层厚度也呈现明显的NE-SW方向的展布特点;受陆缘间歇性浊流的影响,靠构造负载一侧剖面的黑色岩系中出现较多碎屑物质,而真正意义上的硅质岩变少(如图3中的升坪剖面)。随着前陆盆地的继续发展,堆积中心转而向NW方向移动,表现为岩相和生物相突变界面^[43]以及泥盆系与前泥盆系不整合面^[75]自SE向NW层位逐渐升高。

关于形成构造负载或华夏地块抬升的机制,目前仍缺乏充足证据,因此图中并未涉及,但目前从硅质岩的地球化学特征来看,并没有显示出明显的热液活动特征,有可能是造成抬升的构造动力源距研究区较远的原因。华南地块东部在早古生代经历了一次强烈的构造热事件^{[14, 76]①},而岩石圈的热冷却和收缩必然导致区域的沉降,同时造成挠曲强度和沉积载荷的逐渐增加,其沉降范围往往大于拉张期盆缘断裂所限范围^[48],因此对于硅质岩的地球化学特征,热沉降很可能是除构造负载外造成盆地沉降的另一个原因。

8 结 论

硅质岩成因研究表明,湘中南中—晚奥陶世硅质岩以正常海相生物成因为主,形成于大陆边缘背景,相对而言,城步大桥地区的水体较永州岭口更为开阔,仅受间歇性陆源物质输入的影响。

结合等厚度分析以及前人研究成果,本文认为湘中南奥陶纪经历了被动大陆边缘到前陆盆地的转变,这一盆地转变过程在地层学以及硅质岩地球化学特征上得到了很好的响应。

湘中南中—晚奥陶世硅质岩较为一致的地球化学特征指示该时期硅质岩形成于统一盆地中,在硅质岩展布范围内无明显热液影响,暗示造成华夏地块抬升的构造动力源可能还在华南硅质岩展布范围的更南部。

^①龚根辉,陈汉林. 华南早古生代前陆盆地碎屑岩地球化学特征及其地质意义[C]//中国地球科学联合学术年会,2014: 2297-2300.

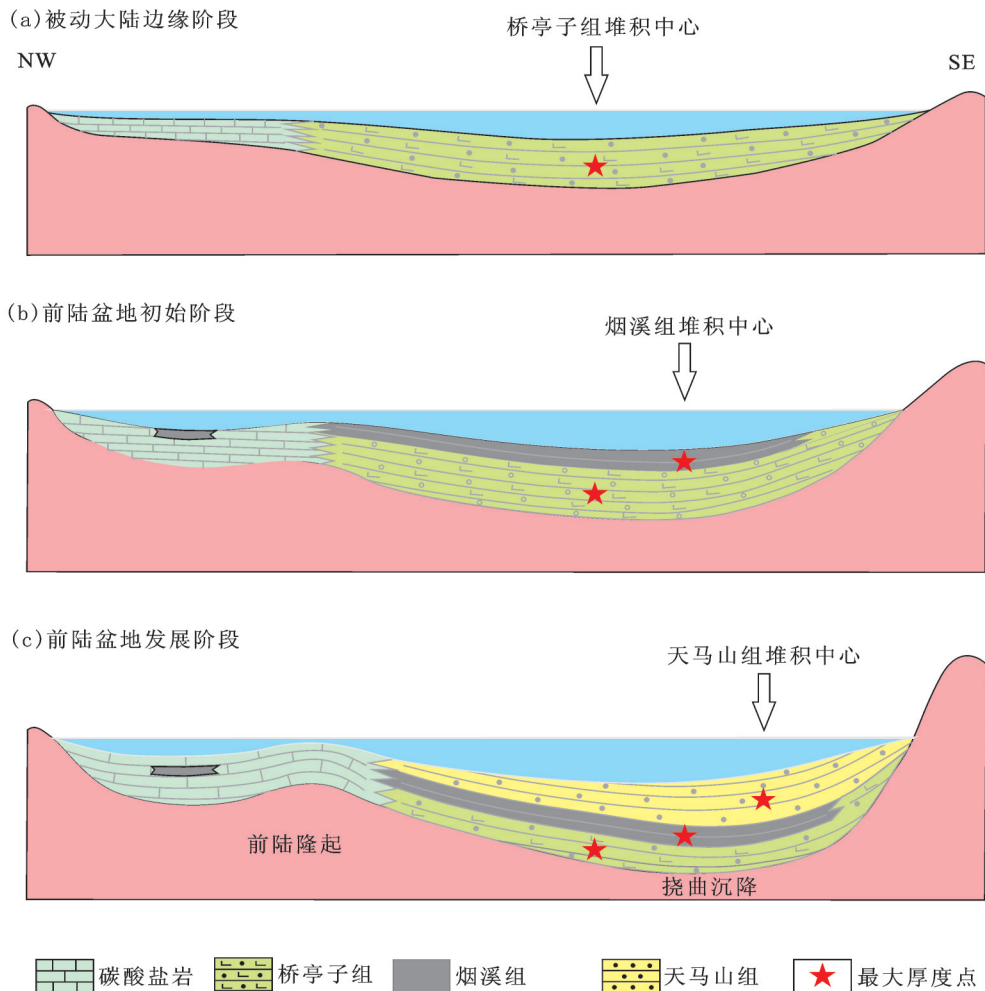


图11湘中南中—晚奥陶世硅质岩系沉积模式及华南奥陶纪盆地演化简图

Fig. 11 Schematic diagram of basin evolution during Ordovician in South China and depositional model of middle-upper Ordovician cherts series in central-southern Hunan

致谢:本文在修改完善过程中得到了武汉地质调查中心田洋、刘浩两位助理研究员的帮助,审稿专家对本文提出了建设性的修改意见,在此一并表示衷心感谢!

参考文献(References):

- [1] 杜远生, 徐亚军. 华南加里东运动初探[J]. 地质科技情报, 2012, 31(5): 43–49.
Du Yuansheng, Xu Yajun. A preliminary study on caledonian event in South China[J]. Geological Science and Technology Information, 2012, 31(5): 43–49(in Chinese with English abstract).
- [2] 舒良树. 华南前泥盆纪构造演化: 从华夏地块到加里东期造山带[J]. 高校地质学报, 2006, 12(4): 418–431.
Shu Liangshu. Predevonian tectonic evolution of South China: From Cathaysian Block to Caledonian period folded orogenic

belt[J]. Geological Journal of China Universities, 2006, 12(4): 418–431(in Chinese with English abstract).

- [3] 刘宝珺. 中国南方古大陆沉积地壳演化与成矿 [M]. 北京: 科学出版社, 1993.
Liu Baojun. Sedimentary Evolution and Mineralization of Ancient Continent in South China[M]. Beijing: Science Press, 1993(in Chinese).
- [4] 王鸿祯. 中国地壳构造发展的主要阶段[J]. 地球科学——中国地质大学学报, 1982, 3: 155–178.
Wang Hongzhen. Main stage of crust structural of China[J]. Earth Science—Journal of China University of Geosciences, 1982, 3: 155–178(in Chinese with English abstract).

- [5] 王鸿祯, 杨巍然, 刘本培. 华南地区古大陆边缘构造史 [M]. 武汉地质学院出版社, 1986.
Wang Hongzhen, Yang Weiran, Liu Benpei. History of Ancient Continental Margin in South China[M]. Wuhan Institute of

- Geology Press, 1986 (in Chinese).
- [6] 殷鸿福, 吴顺宝, 杜远生, 等. 华南是特提斯多岛洋体系的一部 分[J]. 地球科学——中国地质大学学报, 1999, 24(1): 1–12.
Yin HongFu, Wu Shunbao, Du Yuansheng, et al. South China defined as part of Tethyan archipelagic ocean system[J]. Editorial Committee of Earth Science—Journal of China University of Geosciences, 1999, 24(1): 1–12 (in Chinese with English abstract).
- [7] Wang Yuejun, Zhang Feifei, Fan Weiming, et al. Tectonic setting of the South China block in the early Paleozoic: Resolving intracontinental and ocean closure models from detrital zircon U–Pb geochronology[J]. Tectonics, 2010, 29(6).
- [8] 舒良树. 华南构造演化的基本特征[J]. 地质通报, 2012, 31(7): 1035–1053.
Shu Liangshu. An analysis of principal features of tectonic evolution in South China block[J]. Geological Bulletin of China, 2012, 31(7): 1035–1053 (in Chinese with English abstract).
- [9] 张国伟, 郭安林, 王岳军, 等. 中国华南大陆构造与问题[J]. 中国科学 (地球科学), 2013, 43(10): 1553–1582.
Zhang Guowei, Guo Anlin, Wang Yuejun, et al. Tectonics of South China continent and its implications[J]. Science China: Earth Sciences, 2013, 56(11): 1804–1828 (in Chinese).
- [10] Charvet J. The Neoproterozoic–early Paleozoic tectonic evolution of the South China Block: an overview[J]. Journal of Asian Earth Sciences, 2013, 74: 198–209.
- [11] Xu Yajun, Cawood P A, Du Yuansheng, et al. Terminal suturing of Gondwana along the southern margin of South China Craton: Evidence from detrital zircon U–Pb ages and Hf isotopes in Cambrian and Ordovician strata, Hainan Island[J]. Tectonics, 2014, 33(12): 2490–2504.
- [12] Yao Weihua, Li Zhengxiang, Li Wuxian, et al. Detrital provenance evolution of the Ediacaran–Silurian Nanhua foreland basin, South China[J]. Gondwana Research, 2014.
- [13] 何卫红, 唐婷婷, 乐明亮, 等. 华南南华纪一二叠纪沉积大地构造演化[J]. 地球科学——中国地质大学学报, 2014, 39(8): 929–953.
He Weihong, Tang Tingting, Yue Mingliang, et al. Sedimentary and tectonic evolution of Nanhuan–Permian in South China[J]. Earth Science—Journal of China University of Geosciences, 2014, 39(8): 929–953 (in Chinese with English abstract).
- [14] Shu Liangshu, Jahn B M, Charvet J, et al. Early Paleozoic depositional environment and intraplate tectono–magmatism in the Cathaysia Block (South China): Evidence from stratigraphic, structural, geochemical and geochronological investigations[J]. American Journal of Science, 2014, 314(1): 154–186.
- [15] Shu Liangshu, Wang Bo, Cawood P A, et al. Early Paleozoic and early Mesozoic intraplate tectonic and magmatic events in the Cathaysia Block, South China[J]. Tectonics, 2015.
- [16] Adachi M, Yamamoto K, Sugisaki R. Hydrothermal chert and associated siliceous rocks from the northern Pacific: their geological significance as indication od ocean ridge activity[J]. Sedimentary Geology, 1986, 47(1): 125–148.
- [17] Yamamoto K. Geochemical characteristics and depositional environments of cherts and associated rocks in the Franciscan and Shimanto Terranes[J]. Sedimentary Geology, 1987, 52(1): 65–108.
- [18] Murray R W. Chemical criteria to identify the depositional environment of chert: General principles and applications[J]. Sedimentary Geology, 1994, 90(3): 213–232.
- [19] Murray R W, Jones D L, Ten Brink M R B. Diagenetic formation of bedded chert: Evidence from chemistry of the chert–shale couplet[J]. Geology, 1992, 20(3): 271–274.
- [20] Murray R W, Ten Brink M R B, Gerlach D C, et al. Rare earth, major, and trace elements in chert from the Franciscan Complex and Monterey Group, California: Assessing REE sources to fine-grained marine sediments[J]. Geochimica et Cosmochimica Acta, 1991, 55(7): 1875–1895.
- [21] Murray R W, Ten Brink M R B, Gerlach D C, et al. Interceanic variation in the rare earth, major, and trace element depositional chemistry of chert: Perspectives gained from the DSDP and ODP record[J]. Geochimica et Cosmochimica Acta, 1992, 56(5): 1897–1913.
- [22] Murray R W, Ten Brink M R B, Jones D L, et al. Rare earth elements as indicators of different marine depositional environments in chert and shale[J]. Geology, 1990, 18(3): 268–271.
- [23] 张保民, 陈孝红, 危凯, 等. 赣南崇义—永新地区上奥陶统硅质岩地球化学特征及其地质意义[J]. 地质科技情报, 2014, 33(5): 9–15.
Zhang Baomin, Chen Xiaohong, Weikai, et al. Geochemical features of cherts of the upper ordovician in Chongyi–Yongxin area, Southern Jiangxi and their geological significance[J]. Geological Science and Technology Information, 2014, 33(5): 9–15 (in Chinese with English abstract).
- [24] 黄虎, 杜远生, 黄志强, 等. 桂西晚古生代硅质岩地球化学特征及其对右江盆地构造演化的启示[J]. 中国科学: 地球科学, 2013, 53(2): 304–316.
Huang Hu, Du Yuansheng, Huang Zhiqiang, et al. Depositional chemistry of chert during late Paleozoic from western Guangxi and its implication for the tectonic evolution of the Youjiang Basin[J]. Science China: Earth Sciences, 2013, 56(3): 479–493 (in Chinese).
- [25] 黄虎, 杜远生, 杨江海, 等. 水城—紫云—南丹裂陷盆地晚古生代硅质沉积物地球化学特征及其地质意义[J]. 地质学报, 2013, 86(12): 1994–2010.
Huang Hu, Du Yuansheng, Yang Jianghai, et al. Geochemical features of siliceous sediments of the Shuicheng–Ziyun–Nandan rift basin in the late Paleozoic and their tectonic implication[J]. Acta Geologica Sinica, 2013, 86(12): 1994–2010 (in Chinese With English abstract).

- [26] 杜远生, 朱杰, 顾松竹. 北祁连肃南一带奥陶纪硅质岩沉积地球化学特征及其多岛洋构造意义[J]. 地球科学, 2006, 31(1): 101–110.
Du Yuansheng, Zhu Jie, Gu Songzhu. Sedimentary geochemistry and tectonic significance of ordovician cherts in Sunan, North Qilian mountains[J]. Earth Science, 2006, 31(1): 101–110.
- [27] 邓昆, 周立发, 曹欣, 等. 香山群狼嘴子组硅质岩地球化学特征及形成环境[J]. 中国地质, 2007, 34(3): 497–505.
Deng Kun, Zhou Lifan, Cao Xin, et al. Geochemical characteristics and tectonic setting of cherts in the Langzuizi Formation of the Xiangshan Group[J]. Geology in China, 2007, 34(3): 497–505 (in Chinese with English abstract).
- [28] 常华进, 储雪蕾, 冯连君, 等. 湖南安化留茶坡硅质岩的REE地球化学特征及其意义[J]. 中国地质, 2008, 35(5): 879–887.
Chang Huajin, Chu Xuelei, Feng Lianjun, et al. REE geochemistry of the Liuchapo chert in Anhua, Hunan[J]. Geology in China, 2008, 35(5): 879–887 (in Chinese with English abstract).
- [29] 欧莉华, 伊海生, 王刚, 等. 桂西地区乐平统合山组底部海绵骨针硅质岩的发现及古环境意义[J]. 中国地质, 2012, 39(5): 1280–1289.
Ou Lihua, Yi Haisheng, Wang Gang, et al. The discovery of sponge chert on the bottom of the Lopingian Heshan Formation in western Guangxi and its palaeoenvironmental[J]. Geology in China, 2012, 39(5): 1280–1289 (in Chinese with English abstract).
- [30] 柏道远, 周亮, 王先辉, 等. 湘东南南华系—寒武系砂岩地球化学特征及对华南新元古代—早古生代构造背景的制约[J]. 地质学报, 2007, 81(6): 755–771.
Bai Daoyuan, Zhou Liang, Wang Xianhui, et al. Geochemistry of Nanhuan– Cambrian sandstones in southeastern Hunan, and its constraints on Neoproterozoic– early Paleozoic tectonic setting of South China[J]. Acta Geologica Sinica, 2007, 81(6): 755–771 (in Chinese with English abstract).
- [31] Xu YaJun, Du YuanSheng, Cawood P A, et al. Detrital zircon provenance of upper Ordovician and Silurian strata in the northeastern Yangtze block: Response to orogenesis in South China[J]. Sedimentary Geology, 2012, 267: 63–72.
- [32] 尹福光, 许效松. 华南地区加里东期前陆盆地演化过程中的沉积响应[J]. 地球学报, 2001, 22(5): 425–428.
Yin Fuguang, Xu Xiaosong. The sedimentary response to the evolutionary process of Caledonian foreland basin system in South China[J]. Acta Geoscientica Sinica, 2001, 22(5): 425–428 (in Chinese with English abstract).
- [33] 杨明桂, 祝平俊, 熊清华, 等. 新元古代—早古生代华南裂谷系的格局及其演化[J]. 地质学报, 2012, 86(9): 1367–1375.
Yang Minggui, Zhu Pingjun, Xiong Qinghua, et al. Framework and evolution of the Neoproterozoic– early Paleozoic South– China rift system[J]. Acta Geologica Sinica, 2012, 86(9): 1367–1375 (in Chinese with English abstract).
- [34] 张元动, 陈旭. 奥陶纪笔石动物的多样性演变与环境背景[J]. 中国科学: D辑, 2008, 38(1): 10–21.
Zhang Yuandong, Chen Xu. Biodiversity evolution of graptolite and its environment in ordovician[J]. Science China: D Series, 2008, 38(1): 10–21 (in Chinese)
- [35] 李志明, 全秋琦. 中国南部奥陶—志留纪笔石页岩相类型及其构造古地理[J]. 地球科学——中国地质大学学报, 1992, 17(3): 261–269.
Li Zhiming, Quan Qiuqi. Lithofacies types and tectonic palaeogeography of ordovician and silurian graptolite– bearing strata in South China[J]. Earth Science—Journal of China University of Geosciences, 1992, 17(3): 261–269 (in Chinese with English abstract).
- [36] 刘义仁, 傅汉英. 湖南祁东中奥陶世笔石地层[J]. 地质论评, 1985, 31(6): 502–511.
Liu Yiren, Fu Hanying. Graptolite strata of middle ordovician in Qingdong county, Hunan province[J]. Geological Review, 1985, 31(6): 502–511 (in Chinese with English abstract).
- [37] 刘义仁, 傅汉英. 中国奥陶系韩江阶、石口阶的候选层型剖面——湖南祁东双家口剖面(I)[J]. 地层学杂志, 1989, 13(3): 161–192.
Liu Yiren, Fu Hanying. The candidate stratotype section of Hanjing and Shikou stages of Ordovician in China—Shuangjiakou section in Qidong county, Hunan province(I)[J]. Journal of Stratigraphy, 1989, 13(3): 161–192 (in Chinese with English abstract).
- [38] 唐兰, 陈旭, 杨杰, 等. 桂北兴安奥陶纪至志留纪初笔石序列的再研究[J]. 地层学杂志, 2013, 37(1): 1–6.
Tang Lan, Chen Xu, Yang Jie, et al. A restudy of the Ordovician to earliest Silurian graptolite sequence from Xing'an, North Guangxi, China[J]. Journal of Stratigraphy, 2013, 37(1): 1–6 (in Chinese with English abstract).
- [39] 葛祥英, 牟传龙, 周恳恩, 等. 湖南地区晚奥陶世桑比期—凯迪期早期沉积特征及沉积模式[J]. 古地理学报, 2013, (1): 59–68.
Ge Xiangying, Mou Chuanlong, Zhou Kenken, et al. Sedimentary characteristics and depositional model in the Sandbian early Katian ages of late Ordovician in Hunan area[J]. Journal of Palaeogeography, 2013, (1): 59–68 (in Chinese with English abstract).
- [40] 葛祥英, 牟传龙, 周恳恩, 等. 湖南奥陶纪沉积演化特征[J]. 中国地质, 2013, 40(6): 1829–1841.
Ge Xiangying, Mou Chuanlong, Zhou Kenken, et al. Characteristics of Ordovician sedimentary evolution in Hunan province[J]. Geology in China, 2013, 40(6): 1829–1841 (in Chinese with English abstract).
- [41] 罗薇, 何幼斌, 蒋金晶, 等. 湘南地区奥陶系岩石组合及其沉积环境[J]. 地质通报, 2012, 31(7): 1105–1114.
Luo Wei, He Youbin, Jiang Jinjing, et al. An analysis of Ordovician rock association and sedimentary environment in southern Hunan Province [J]. Geological Bulletin of China, 2012,

- 31(7): 1105–1114(in Chinese with English abstract).
- [42] 蒋德和, 杨振强. 湘中地区中奥陶统沉积岩的稀土元素地球化学[J]. 沉积学报, 1994, 12(1): 106–111.
Jiang Dehe, Yang Zhenqiang. REE Geochemistry of sedimentary rocks middle Ordovician in central Hunan Province[J]. *Acta Sedimentologica Sinica*, 1994, 12(1): 106–111(in Chinese with English abstract).
- [43] 陈旭, 樊隽轩, 陈清, 等. 论广西运动的阶段性[J]. 中国科学: 地球科学, 2014, 44(5): 842–850.
Chen Xu, Fan Junxuan, Chen Qing, et al. Toward a stepwise Kwangssian orogeny[J]. *Science China: Earth Sciences*, 2014, 44(5): 842–850(in Chinese).
- [44] 陈旭, 张元动, 樊隽轩, 等. 广西运动的进程: 来自生物相和岩相带的证据[J]. 中国科学: 地球科学, 2012, 42(11): 1617–1626.
Chen Xu, Zhang Yuandong, Fan Junxuan, et al. Onset of the Kwangssian orogeny as evidenced by biofacies and lithofacies[J]. *Science China: Earth Sciences*, 2012, 42(11): 1617–1626(in Chinese).
- [45] 赵俊峰, 刘池洋, 喻林, 等. 鄂尔多斯盆地中生代沉积和堆积中心迁移及其地质意义[J]. 地质学报, 2008, 82(4): 540–552.
Zhao Junfeng, Liu Chiayang, Yu lin, et al. The transfer of depocenters and accumulation centers of Ordos basin in Mesozoic and its meaning[J]. *Acta Geologica Sinica*, 2008, 82(4): 540–552 (in Chinese with English abstract).
- [46] 曹红霞, 李文厚, 陈全红, 等. 鄂尔多斯盆地南部晚三叠世沉降与沉积中心研究[J]. 大地构造与成矿学, 2008, 32(2): 159–164.
Cao Hongxia, Li Wenhui, Chen Quanhong, et al. Center of late Triassic subsidence and depocenter for the southern Ordos basin[J]. *Geotectonica et metallogenesis*, 2008, 32(2): 159–164 (in Chinese with English abstract).
- [47] 吕红华, 周祖翼. 前陆盆地陆源沉积序列的特征与成因机制[J]. 地球科学进展, 2010, 25(7): 706–714.
Lv Honghua, Zhou Zuyi. Characteristics and genesis of terrigenous depositional sequences in foreland basins[J]. *Advances in Earth Science*, 2010, 25(7): 706–714(in Chinese with English abstract).
- [48] 解习农, 陆永潮. 陆相盆地幕式构造旋回与层序构成[J]. 地球科学: 中国地质大学学报, 1996, 21(1): 27–33.
Xie Xinong, Lu Yongchao. Episodic tectonic cycles and internal architectures of sequences in continental basin [J]. *Earth Science—Journal of China University of Geosciences*, 1996, 21(1): 27–33 (in Chinese with English abstract).
- [49] 广西壮族自治区地质矿产局. 广西壮族自治区区域地质志[M]. 北京: 地质出版社, 1985.
Guangxi Bureau of Geology & Mineral Prospecting & Exploitation[M]. Beijing: Geological Publishing House, 1985(in Chinese).
- [50] 江西省地质矿产局. 江西省区域地质志[M]. 北京: 地质出版社, 1984.
- Bureau of Geology and Mineral Exploration and Development of Jiangxi Province[M]. Beijing: Geological Publishing House, 1984 (in Chinese).
- [51] McLennan S. Rare earth elements in sedimentary rocks: Influence of provenance and sedimentary processes[J]. *Reviews in Mineralogy and Geochemistry*, 1989, 21(1): 169–200.
- [52] Bostrom M K, Peterson M. The origin of aluminum-poor ferromanganese sediments in areas of high heat flow on the East Pacific Rise[J]. *Marine Geology*, 1969, 7(5): 427–447.
- [53] Sugisaki R, Yamamoto K, Adachi M. Triassic bedded cherts in central Japan are not pelagic[J]. *Nature*, 1982, 298(5875): 644–647.
- [54] 王博, 舒良树. 对赣东北晚古生代放射虫的初步认识[J]. 地质论评, 2001, 47(4): 337–344.
Wang Bo, Shu Liangshu. Notes on Late Paleozoic Radiolarians of Northeastern Jiangxi Province[J]. *Geological Review*, 2001, 47(4): 337–344(in Chinese with English abstract).
- [55] 郑宁, 宋天锐, 李廷栋, 等. 华南造山带下寒武统和中奥陶统发现放射虫[J]. 中国地质, 2012, 39(1): 260–265.
Zheng Ning, Song Tianrui, Li Tingdong, et al. The discovery of the Lower Cambrian and Middle Ordovician Radiolaria in the South China orogenic belt[J]. *Geology in China*, 2012, 39(1): 260–265(in Chinese with English abstract).
- [56] Taylor S R, McLennan S M. The Continental Crust: Its Composition and Evolution[M]. Oxford: Blackwell Scientific Publications, 1985: 9–56.
- [57] Sugitani K, Horiuchi Y, Adachi M, et al. Anomalously low $\text{Al}_2\text{O}_3/\text{TiO}_2$ values for Archean cherts from the Pilbara block, western Australia—possible evidence for extensive chemical weathering on the early earth[J]. *Precambrian Research*, 1996, 80(1): 49–76.
- [58] Hayashi KI, Fujisawa H, Holland H D, et al. Geochemistry of 1.9 Ga sedimentary rocks from northeastern Labrador, Canada[J]. *Geochimica et Cosmochimica Acta*, 1997, 61(19): 4115–4137.
- [59] Sholkovitz E R. Rare-earth elements in marine sediments and geochemical standards[J]. *Chemical Geology*, 1990, 88(3): 333–347.
- [60] Kamber B S, Greig A, Collerson K D. A new estimate for the composition of weathered young upper continental crust from alluvial sediments, Queensland, Australia[J]. *Geochimica et Cosmochimica Acta*, 2005, 69(4): 1041–1058.
- [61] Bau M, Koschinsky A, Dulski P, et al. Comparison of the partitioning behaviours of yttrium, rare earth elements, and titanium between hydrogenetic marine ferromanganese crusts and seawater[J]. *Geochimica et Cosmochimica Acta*, 1996, 60(10): 1709–1725.
- [62] Zhang J, Amakawa H, Nozaki Y. The comparative behaviors of yttrium and lanthanides in the seawater of the North Pacific[J]. *Geophysical Research Letters*, 1994, 21(24): 2677–2680.

- [63] Nozaki Y, Zhang J, Amakawa H. The fractionation between Y and Ho in the marine environment[J]. *Earth and Planetary Science Letters*, 1997, 148(1): 329–340.
- [64] Lawrence M G, Greig A, Collerson K D, et al. Rare earth element and yttrium variability in South East Queensland waterways[J]. *Aquatic Geochemistry*, 2006, 12(1): 39–72.
- [65] Nozaki Y, Lerche D, Alibo D S, et al. The estuarine geochemistry of rare earth elements and indium in the Chao Phraya River, Thailand[J]. *Geochimica et Cosmochimica Acta*, 2000, 64(23): 3983–3994.
- [66] Ohta A, Ishii S, Sakakibara M, et al. Systematic correlation of the Ce anomaly with the Co/(Ni+ Cu) ratio and Y fractionation from Ho in distinct types of Pacific deep-sea nodules[J]. *Geochem J*, 1999, 33: 399–417.
- [67] Kato Y, Nakao K, Isozaki Y. Geochemistry of Late Permian to Early Triassic pelagic cherts from southwest Japan: implications for an oceanic redox change[J]. *Chemical Geology*, 2002, 182(1): 15–34.
- [68] Kametaka M, Takebe M, Nagai H, et al. Sedimentary environments of the Middle Permian phosphorite–chert complex from the northeastern Yangtze platform, China; the Gufeng Formation: a continental shelf radiolarian chert[J]. *Sedimentary Geology*, 2005, 174(3): 197–222.
- [69] Girty G H, Ridge D L, Knaack C, et al. Provenance and depositional setting of Paleozoic chert and argillite, Sierra Nevada, California[J]. *Journal of Sedimentary Research*, 1996, 66 (1): 107–118.
- [70] 周小进, 杨帆. 中国南方新元古代—早古生代构造演化与盆地原型分析[J]. 石油实验地质, 2009, 31(2): 128–141.
- Zhou Xiaojin, Yang Fan. Tectonic Evolution and prototypes analysis from neoproterozoic to early paleozoic in South China [J]. *Petroleum Geology & Experiment*, 2009, 31(2): 128–141 (in Chinese with English abstract).
- [71] 王清晨, 蔡立国. 中国南方显生宙大地构造演化简史[J]. *地质学报*, 2007, 81(8): 1025–1040.
- Wang Qingchen, Cai Liguo. Phanerozoic tectonic evolution of South China[J]. *Acta Geologica Sinica*, 2007, 81(8): 1025–1040 (in Chinese with English abstract).
- [72] 陈洪德, 侯明才, 许效松, 等. 加里东期华南的盆地演化与层序格架[J]. 成都理工大学学报: 自然科学版, 2006, 33(1): 1–8 (in Chinese with English abstract).
- Chen Hongde, Hou Mingcai, Xu Xiaosong, et al. Tectonic evolution and sequence stratigraphic framework in South China during Caledonian[J]. *Journal of Chengdu University of Technology (Science & Technology Edition)*, 2006, 33(1): 1–8 (in Chinese with English abstract).
- [73] 熊江宇, 詹任宾, 徐红根, 等. 通过奥陶纪–志留纪过渡带扩张的卡他西亚老陆地: 出现的证据和可能的动力学[J]. *中国科学: 地球科学*, 2010, 53(1): 1–17.
- Rong Jiayu, Zhan Renbin, Xu Honggen, et al. Expansion of the Cathaysian Oldland through the Ordovician–Silurian transition: Emerging evidence and possible dynamics[J]. *Science in China Series D: Earth Sciences*, 2010, 53(1): 1–17.
- [74] 熊江宇, 王毅, 张晓奥. 通过奥陶纪–志留纪过渡带浅海红色页岩追踪: 上扬子地区志留系下统红色页岩[J]. *科学通报*, 2012, 55(5): 699–713.
- Rong Jiayu, Wang Yi, Zhang Xiaole. Tracking shallow marine red beds through geological time as exemplified by the lower Telychian (Silurian) in the Upper Yangtze Region, South China[J]. *Science China Earth Sciences*, 2012, 55(5): 699–713.
- [75] 徐勇, 卡伍德 P A, 杜宇, 等. 通过南中国北部边缘带构造演化约束的古生代造山运动[J]. *Tectonophysics*, 2014, 636: 40–51.
- Xu Y, Cawood P A, Du Y, et al. Early Paleozoic orogenesis along Gondwana's northern margin constrained by provenance data from South China[J]. *Tectonophysics*, 2014, 636: 40–51.
- [76] 李正祥, 李献华, 卫厚 JA, 等. 通过早古生代吴夷–云开造山运动约束的南中国东南部构造演化[J]. *美国地质学会会刊*, 2010, 122(5–6): 772–793.